



**Multivariate Quantiles: Geometric and
Measure-Transportation-Based Contours**

Marc Hallin
ECARES, and Département de Mathématique,
Université libre de Bruxelles

Dimitri Konen
ECARES, and Département de Mathématique,
Université libre de Bruxelles

October 2023

ECARES working paper 2023-14

Multivariate Quantiles: Geometric and Measure-Transportation-Based Contours

Marc Hallin and Dimitri Konen

Abstract Quantiles are a fundamental concept in probability and theoretical statistics and a daily tool in their applications. While the univariate concept of quantiles is quite clear and well understood, its multivariate extension is more problematic. After half a century of continued efforts and many proposals, two concepts, essentially, are emerging: the so-called (*relabelled*) *geometric quantiles*, extending the characterization of univariate quantiles as minimizers of an L_1 loss function involving the *check functions*, and the more recent *center-outward quantiles* based on measure transportation ideas. These two concepts yield distinct families of *quantile regions* and *quantile contours*. Our objective here is to present a comparison of their main theoretical properties and a numerical investigation of their differences.

1 Introduction

Quantiles are a fundamental concept in probability and theoretical statistics and a familiar tool in their applications, ranging from descriptive statistics and data analysis to statistical inference. The univariate concept of a quantile function (the inverse of a distribution function) is well understood and well studied in dimension $d = 1$. Despite half a century of efforts, however, the multivariate extension (dimension $d \geq 2$) of this essential notion remains quite problematic—the obvious difficulty being the absence of a canonical ordering of the real space for dimension two and higher.

Various proposals have been made in the literature, none of which is fully agreed upon. Two concepts, essentially, are emerging from these many attempts: the so-called (*relabelled*) *geometric quantiles* (Chaudhuri 1996), extending the characterization of univariate quantiles as minimizers of an L_1 loss function involving the

Marc Hallin and Dimitri Konen
Université libre de Bruxelles, Belgium, and University of Warwick, United Kingdom
e-mail: mhallin@ulb.be, dimitri.konen@warwick.ac.uk

check functions, and the more recent *center-outward quantiles* (Hallin et al. 2021) based on measure transportation ideas.

The objective of this note is a brief comparison of some of the properties of the quantile regions and quantile contours associated with these two concepts.

2 Quantiles: from univariate to multivariate

Throughout, the inner product of two vectors $x, y \in \mathbb{R}^d$ is denoted as $x'y$; \mathbb{B}_d and \mathbb{S}^{d-1} stand for the open unit ball and the $(d-1)$ -dimensional unit sphere, respectively, in \mathbb{R}^d .

2.1 Definitions and basic properties

Let X denote a Lebesgue-absolutely continuous real-valued random variable with distribution P over \mathbb{R} and distribution function

$$F_P : x \mapsto F_P(x) := P(X \leq x).$$

To simplify the exposition, assume that X admits a nonvanishing density $f := dP/d\lambda$ with respect to the Lebesgue measure λ so that, in particular, F_P is continuous and strictly monotone increasing, hence invertible. The quantile function of P (equivalently, the quantile function of $X \sim P$) then is defined as the inverse $Q_P := F_P^{-1}$ of the distribution function F_P and the quantile of order $\alpha \in (0, 1)$ of P (of $X \sim P$) is the value $Q_P(\alpha)$ of Q_P at α .

Along with quantiles of given order $\alpha \in (0, 1)$, it is often convenient to consider central quantile regions and contours. In dimension $d = 1$, call *quantile region of order $\tau \in [0, 1)$* of P (of $X \sim P$) the closed interval

$$\mathcal{R}_P(\tau) := \left[Q_P\left(\frac{1-\tau}{2}\right), Q_P\left(\frac{1+\tau}{2}\right) \right]$$

(an interquantile interval) and *quantile contour of order τ* of P (of $X \sim P$) the boundary

$$\mathcal{C}_P(\tau) := \left\{ Q_P\left(\frac{1-\tau}{2}\right), Q_P\left(\frac{1+\tau}{2}\right) \right\}$$

of $\mathcal{R}_P(\tau)$.

The quantile region of order 0 is the degenerate interval $\mathcal{R}_P(0) = \{Q_P(1/2)\}$ and has Lebesgue measure zero: call it the *median region*. Similarly, the quantile region of order 1/2 is the traditional interquartile interval: $\mathcal{R}_P(1/2) = [Q_P(1/4), Q_P(3/4)]$. Contrary to the quantile halflines $(-\infty, Q_P(\alpha)]$, which very much depend on the orientation of the real line (an orientation that is no longer meaningful in \mathbb{R}^d for $d \geq 2$), the concepts of quantile regions and contours of order τ are “center-

outward” concepts (the “center” being the median $Q_P(1/2)$) and are invariant under a change of the orientation of \mathbb{R} (an orthogonal transformation). The collection $\{\mathcal{R}_P(\tau) : \tau \in [0, 1]\}$ of quantile regions is strictly nested (in the sense of set inclusion) as τ ranges from zero to one, with $\mathcal{R}_P(0) = \bigcap_{\tau \in [0, 1]} \mathcal{R}_P(\tau)$. It is easily seen that $\mathcal{C}_P(|2F_P(x) - 1|)$ is the unique quantile contour running through $x \in \mathbb{R}$; actually,

$$\mathcal{R}_P(\tau) = \{x : |2F_P(x) - 1| \leq \tau\} \quad \text{and} \quad \mathcal{C}_P(\tau) = \{x : |2F_P(x) - 1| = \tau\} \quad \tau \in [0, 1]. \quad (1)$$

An essential property of a quantile function is that the P-probability content of a quantile region $\mathcal{R}_P(\tau)$ is τ irrespective of P: namely, $P(\mathcal{R}_P(\tau)) = \tau$ for all P. What would be the relevance, indeed, of an interquartile region $\mathcal{R}_P(1/2)$ with probability content 0.5 under $P = P_1$ (as should be) but probability content 0.6 under $P = P_2$, and probability content 0.7 under $P = P_3$? This property, in dimension $d = 1$, is equivalent to the property of $F_P(X)$ being uniform over $[0, 1)$ for $X \sim P$.

When the center-outward quantile regions $\mathcal{R}_P(\tau)$ and contours $\mathcal{C}_P(\tau)$ are the main points of interest, it is natural to replace F_P and Q_P by center-outward counterparts: call $F_P^\pm := 2F_P - 1$ and $Q_P^\pm := (F_P^\pm)^{-1}$ the *center-outward distribution* and *quantile functions* of P (or $X \sim P$), respectively. Just like F_P and Q_P , the maps F_P^\pm and Q_P^\pm are monotone increasing and carry the same information about P, which they fully characterize. Instead of being uniformly distributed over $[0, 1)$, $F_P^\pm(X)$, when $X \sim P$, is uniform over $(-1, 1)$, which is the open unit ball \mathbb{B}_1 in \mathbb{R} . In fact, denoting by U_1 the uniform distribution over \mathbb{B}_1 , we have $F_P^\pm(X) \sim U_1$ when $X \sim P$, hence $Q_P^\pm(U) \sim P$ if $U \sim U_1$. In the terminology of measure transportation, we say that the *transport* F_P^\pm is *pushing P forward to* U_1 and that its inverse Q_P^\pm is *pushing* U_1 *forward to* P, which we conveniently denote as

$$F_P^\pm \# P = U_1 \quad \text{and} \quad Q_P^\pm \# U_1 = P,$$

respectively. The quantile region $\mathcal{R}_P(\tau)$ and quantile contour $\mathcal{C}_P(\tau)$ then take the simple forms (equivalent to (1))

$$\mathcal{R}_P(\tau) = Q_P^\pm(\tau \mathbb{B}_1) \quad \text{and} \quad \mathcal{C}_P(\tau) = Q_P^\pm(\tau \mathbb{S}^0), \quad \tau \in [0, 1), \quad (2)$$

respectively, where $\mathbb{S}^0 := \{-1, 1\}$ stands for the (0-dimensional) unit sphere in \mathbb{R} .

2.2 Characterization of univariate quantiles as minimizers of expected check functions

When P is a probability measure over \mathbb{R} and $X \sim P$, and given a level $\alpha \in [0, 1)$, a quantile of order α of X , by definition, is any $x \in \mathbb{R}$ satisfying

$$P(X < x) \leq \alpha \leq P(X \leq x).$$

It turns out that such x 's are exactly the minimizers (with respect to $\theta \in \mathbb{R}$) of the objective function

$$\theta \mapsto M_\alpha^P(\theta) := \mathbb{E}_P[\rho_\alpha(\theta - X) - \rho_\alpha(X)] \quad (3)$$

where, denoting by z^+ and z^- the positive and negative parts, respectively, of $z \in \mathbb{R}$,

$$\rho_\alpha : z \mapsto \rho_\alpha(z) := |z| + (2\alpha - 1)z = 2\{\alpha z^+ + (1 - \alpha)z^-\}, \quad z \in \mathbb{R}, \alpha \in [0, 1)$$

stands for the so-called *check function*. Noting that $M_\alpha^P(\theta)$ rewrites as

$$M_\alpha^P(\theta) = \mathbb{E}_P[|\theta - X| - |X|] - (2\alpha - 1)\theta \quad (4)$$

for all $\theta \in \mathbb{R}$, it follows from the triangular inequality that $||X - \theta| - |X|| \leq |\theta|$, which is integrable. The objective function M_α^P , hence the correspondence between quantiles and the minimizing procedure in (3), thus remains well defined for an *arbitrary* probability measure P , without any moment assumption. In this general setting, we have, even in the absence of a finite moment of order one,

$$Q_P(\alpha) = \operatorname{argmin}_{\theta \in \mathbb{R}} M_\alpha^P(\theta), \quad \alpha \in [0, 1).$$

For $\alpha = 0.5$, $M_\alpha^P(\theta) = \mathbb{E}_P[|\theta - X| - |X|]$; in case $\mathbb{E}_P(X) < \infty$, thus, we recover the familiar characterization of the median $Q_P(1/2)$ as an L_1 location parameter, the minimizer of the expected absolute deviation $\mathbb{E}_P[|\theta - X|]$.

Recalling that $F_P^\pm := 2F_P - 1$, we see that the natural labeling for center-outward quantiles is provided by $\beta := 2\alpha - 1 \in (-1, 1)$. Therefore, the center-outward version of the characterization of quantiles as minimizers is obtained by relabeling $2\alpha - 1$ as β in (3). This leads to the characterization of center-outward quantiles $Q_P^\pm(\beta)$ as minimizers with respect to $\theta \in \mathbb{R}$ of the objective function

$$\theta \mapsto O_\beta^P(\theta) := \mathbb{E}_P[|\theta - X| - |X|] - \beta\theta, \quad \beta \in (-1, 1). \quad (5)$$

We then have (still, without any moment assumption)

$$Q_P^\pm(\beta) = \operatorname{argmin}_{\theta \in \mathbb{R}} O_\beta^P(\theta), \quad \beta \in (-1, 1).$$

The value $\beta = 0$ yields the median $Q_P^\pm(0) = Q_P(1/2)$ of P , while positive (resp. negative) values of β are associated to quantiles sitting to the right-hand (resp. left-hand) side of the median.

2.3 Characterization of univariate quantile functions as monotone transports

Consider a probability measure P with non-vanishing density f with respect to the Lebesgue measure on \mathbb{R} . An alternative to the characterization, in dimension $d = 1$, of Q_P^\pm (hence of Q_P and F_P^\pm) as minimizers of expected check functions is obtained by noting that Q_P^\pm is monotone increasing and pushes U_1 forward to P . This fully characterizes Q_P^\pm up to a set of values with Lebesgue measure zero.¹ The center-outward quantile function Q_P^\pm , thus, can be characterized as the almost everywhere unique monotone map from the open unit ball $\mathbb{B}_1 = (-1, 1)$ to \mathbb{R} such that $Q_P^\pm \# U_1 = P$.

3 Multivariate quantile functions, regions, and contours

Extending to dimension $d > 1$ the characterizations of quantile functions developed in Section 2.2 leads to the concept of *geometric quantiles* first proposed by Chaudhuri (1996) while the measure-transportation-based characterization developed in Section 2.3 leads to the concept of multivariate *center-outward quantiles* proposed in Hallin et al. (2021).

3.1 Geometric quantiles and geometric quantile contours

Consider a probability measure P supported on \mathbb{R}^d , with $d \geq 2$. Extending to a d -dimensional framework the characterization of univariate quantiles as minimizers of expected check functions is obtained by replacing, in (5), the absolute values with Euclidean norms and $\beta \in (-1, 1) = \mathbb{B}_1$ with $\mathbf{v} \in \mathbb{B}_d$. Letting $\mathbf{v} =: \tau \mathbf{u} \in \mathbb{B}_d$ with $\tau = \|\mathbf{v}\| \in (0, 1)$ and $\mathbf{u} = \mathbf{v}/\|\mathbf{v}\| \in \mathbb{S}^{d-1}$, define the *geometric quantile* of order $\tau > 0$ in direction $\mathbf{u} = \mathbf{v}/\|\mathbf{v}\|$ of P (of $\mathbf{X} \sim P$) as an arbitrary minimizer, over $\mathbf{z} \in \mathbb{R}^d$, of the objective function

$$\mathbf{z} \mapsto O_{\tau, \mathbf{u}}^P(\mathbf{z}) := E_P[\|\mathbf{z} - \mathbf{X}\| - \|\mathbf{X}\|] - \tau \mathbf{u}' \mathbf{z} \quad (6)$$

where $\mathbf{X} \sim P$; throughout, boldface is used to stress that the variables take values in \mathbb{R}^d . The objective function $O_{\tau, \mathbf{u}}^P$ being convex, it can be shown that the geometric quantiles of P are unique as soon as P is not supported on a single line of \mathbb{R}^d —a situation which essentially boils down to a univariate setting: see Theorem 1 in Paidaveine and Virta (2020) for a discussion. For $\tau = 0$, define the geometric me-

¹ As we shall see, the existence and (almost everywhere) uniqueness, in dimension $d = 1$, of a monotone non-decreasing mapping (that is, the derivative, hence the gradient, of a convex function) pushing U_1 forward to P is a particular case of a famous and more general measure transportation result by McCann (1995).

dian as the minimizer of $E_P[\|\mathbf{z} - \mathbf{X}\| - \|\mathbf{X}\|]$ which, still in view of the triangular inequality, exists without any moment assumption and is better known as the *Fréchet median*.

When uniqueness holds (P not supported on a line), we denote by $\mathbf{Q}_P^g(\tau\mathbf{u})$ the geometric quantile of order $\tau \in [0, 1)$ in direction \mathbf{u} of P (of $\mathbf{X} \sim P$) and by $\mathbf{Q}_P^g(\mathbf{0})$ the geometric or Fréchet median, which can be interpreted as the geometric quantile of order $\tau = 0$ in any direction \mathbf{u} . Here again, boldface is used to stress that \mathbf{Q}_P^g takes values in \mathbb{R}^d .

Strongly related to the gradient of $O_{\tau, \mathbf{u}}^P$, we define the *geometric distribution function* \mathbf{F}_P^g of P as the mapping

$$\mathbf{z} \mapsto \mathbf{F}_P^g(\mathbf{z}) := E_P \left[\frac{\mathbf{z} - \mathbf{X}}{\|\mathbf{z} - \mathbf{X}\|} \mathbb{1}[\mathbf{X} \neq \mathbf{z}] \right], \quad \mathbf{z} \in \mathbb{R}^d, \quad (7)$$

where $\mathbb{1}[A]$ stands for the indicator function of A . While the definition of \mathbf{Q}_P^g is motivated by the characterization of univariate center-outward quantiles as minimizers of an objective function, let us stress that the geometric distribution function in (7) is a natural analogue of the univariate center-outward distribution as well. Indeed, recalling that, for $d = 1$, $F_P^\pm := 2F_P - 1$ and observing that $2\mathbb{1}[X \leq z] - 1 = \text{sign}(z - X)$, one obtains

$$F_P^\pm(z) = E_P[\text{sign}(z - X)], \quad z \in \mathbb{R}, \quad (8)$$

to which \mathbf{F}_P^g in (7) reduces when $d = 1$. The direction $(\mathbf{z} - \mathbf{X})/\|\mathbf{z} - \mathbf{X}\|$, thus, can be interpreted as a multivariate sign for $\mathbf{z} - \mathbf{X} \neq \mathbf{0}$.

Provided that P is non-atomic and is not supported on a single line of \mathbb{R}^d , Theorem 6.2 in Konen and Paindaveine (2022) entails that \mathbf{F}_P^g is a homeomorphism between \mathbb{R}^d and the open unit ball \mathbb{B}_d of \mathbb{R}^d , with inverse \mathbf{Q}_P^g . Consequently, one also can define \mathbf{Q}_P^g as $(\mathbf{F}_P^g)^{-1}$ with \mathbf{F}_P^g defined in (7), or define \mathbf{F}_P^g as $(\mathbf{Q}_P^g)^{-1}$ with \mathbf{Q}_P^g defined as the minimizer of $O_{\tau, \mathbf{u}}^P$ in (6). Further results about the regularity of \mathbf{F}_P^g and \mathbf{Q}_P^g are provided in Konen (2022).

With this, one can define *geometric quantile regions* and *contours*, which are multivariate extensions of the univariate center-outward quantile regions and contours, by letting

$$\mathcal{R}_P^g(\tau) := \mathbf{Q}_P^g(\tau\mathbb{B}_d) \quad \text{and} \quad \mathcal{C}_P^g(\tau) := \mathbf{Q}_P^g(\tau\mathbb{S}^{d-1}), \quad \tau \in [0, 1). \quad (9)$$

For $\tau = 0$, $\mathcal{R}_P^g(0)$ and $\mathcal{C}_P^g(0)$ reduce to the singlepoint set consisting of the *geometric* or *Fréchet median*; as in the univariate case, the geometric median is an L_1 location parameter that minimizes, when finite first-order moments exist, the expected absolute deviation (*absolute deviations*, here, are to be understood as *Euclidean norms* of deviations).

3.2 Measure-transportation-based quantiles and quantile contours

Denote by U_d the spherical uniform over the open unit ball \mathbb{B}_d , that is, the product of a uniform distribution over the unit sphere \mathbb{S}^{d-1} and a (univariate) uniform over the distances from the origin; in other words, U_d is the probability measure with density $f_{U_d}(\mathbf{x})$ proportional to $1/\|\mathbf{x}\|^{d-1} \mathbb{1}[\mathbf{0} < \|\mathbf{x}\| \leq 1]$ for $\mathbf{0} < \|\mathbf{x}\|$ and $f_{U_d}(\mathbf{0}) = \infty$.

A celebrated result by McCann (1995) implies that, for any distribution P over \mathbb{R}^d , there exists an almost everywhere unique gradient of a convex function pushing P forward to the spherical uniform U_d over the (open) unit ball \mathbb{B}_d of \mathbb{R}^d . In dimension $d = 1$, a gradient of convex function is a monotone non-decreasing function and the unique monotone non-decreasing function pushing P forward to U_1 is the center-outward distribution function $F_P^\pm := 2F_P - 1$. For arbitrary dimension $d \geq 1$, this leads Hallin et al. (2021) to define the *center-outward distribution function* of P (or $\mathbf{X} \sim P$) as the almost everywhere unique gradient of a convex function \mathbf{F}_P^\pm pushing P to the spherical uniform U_d .

Assuming that P belongs to the class \mathcal{P}_d^+ of Lebesgue-absolutely continuous distributions with density bounded away from zero and infinity on any compact² subset of \mathbb{R}^d , Figalli (2018) showed that \mathbf{F}_P^\pm is a homeomorphism between $\mathbb{R}^d \setminus (\mathbf{F}_P^\pm)^{-1}(\mathbf{0})$ and the punctured unit ball $\mathbb{B}_d \setminus \{\mathbf{0}\}$. The restriction of \mathbf{F}_P^\pm to $\mathbb{R}^d \setminus (\mathbf{F}_P^\pm)^{-1}(\mathbf{0})$ is thus continuously invertible. We call its (continuous) inverse $\mathbf{Q}_P^\pm := (\mathbf{F}_P^\pm)^{-1}$ the *center-outward quantile function* of P (or $\mathbf{X} \sim P$). This yields *center-outward quantile regions* and *contours*, of order τ which are multivariate extensions of the univariate center-outward quantile regions and contours defined in (2), of the form

$$\mathcal{R}_P^\pm(\tau) := \mathbf{Q}_P^\pm(\tau \mathbb{B}_d) \quad \text{and} \quad \mathcal{C}_P^\pm(\tau) := \mathbf{Q}_P^\pm(\tau \mathbb{S}^{d-1}), \quad \tau \in (0, 1), \quad (10)$$

respectively. As for $\tau = 0$, define $\mathcal{R}_P^\pm(0) := \bigcap_{0 < \tau < 1} \mathcal{R}_P^\pm(\tau)$ as the *center-outward median region*, which is shown to be convex and compact, with Hausdorff dimension at most $d - 1$ (Figalli, 2018). Note the parallel between (10) and (9).

4 Main properties

4.1 Geometric quantile regions and contours

Consider a probability measure P which is non-atomic and is not supported on a single line of \mathbb{R}^d ; in particular, \mathbf{F}_P^g and \mathbf{Q}_P^g are homeomorphisms with $\mathbf{Q}_P^g = (\mathbf{F}_P^g)^{-1}$. Then, geometric quantile regions and contours have the following topological properties:

² Formally, for any compact subset $K \subset \mathbb{R}^d$, there exist constants $0 < c_K^- \leq c_K^+ < \infty$ such that $c_K^- \leq dP/d\lambda(\mathbf{x}) \leq c_K^+$ for all $\mathbf{x} \in K$. This assumption is maintained here for clarity of exposition, but it can be relaxed: see del Barrio et al. (2020) and del Barrio and González-Sanz (2023).

- (i) the regions $\mathcal{R}_P^g(\tau)$ are compact and arc-connected for all $\tau \in [0, 1)$;
- (ii) the regions $\mathcal{R}_P^g(\tau)$ are strictly nested as τ increases: for any $0 \leq \tau_1 < \tau_2 < 1$, we have $\mathcal{R}_P^g(\tau_1) \subsetneq \mathcal{R}_P^g(\tau_2)$;
- (iii) if P has a bounded density f , then the contour $\mathcal{C}_P^g(\tau)$ is a $(d-1)$ -dimensional manifold of class C^{d-1} for all $\tau \in (0, 1)$; if, in addition, f is of class $C^{k,\alpha}$ for some $k \in \mathbb{N}$ and $\alpha \in (0, 1)$, then $\mathcal{C}_P^g(\tau)$ is of class C^{d+k} for all $\tau \in (0, 1)$;
- (iv) for $d = 1$, \mathbf{F}_P^g , \mathbf{Q}_P^g , \mathcal{R}_P^g , and \mathcal{C}_P^g reduce to F_P^\pm , Q_P^\pm , \mathcal{R}_P^\pm , and \mathcal{C}_P^\pm .

While properties (i)-(ii) are straightforward consequences of the continuity of \mathbf{Q}_P^g , property (iii) requires more advanced mathematical tools. That property was established in Konen (2022), where it is shown that geometric distribution functions satisfy a linear partial differential equation, which was the key to the derivation of the regularity properties of geometric contours. Among other things, this PDE implies that geometric distribution functions fully characterize *arbitrary* probability measures (no moment or non-atomicity assumptions required), namely,

- (v) if P_1 and P_2 are *arbitrary* probability measures such that $\mathbf{F}_{P_1}^g = \mathbf{F}_{P_2}^g$, then $P_1 = P_2$.

This characterization result has been long known, though: the first proof was provided in Theorem 2.5 of Koltchinski (1997) and was refined recently in Konen (2022).

Geometric quantile and distribution functions further enjoy the following natural equivariance properties; see Girard and Stupfler (2017) and Konen and Paindaveine (2022).

- (vi) Let $\theta \in \mathbb{R}^d$ and denote by \mathbf{O} an arbitrary $d \times d$ orthogonal matrix. For $\mathbf{X} \sim P$, write $\mathbf{F}_X^g, \mathbf{F}_X^g$, etc. instead of $\mathbf{F}_P^g, \mathbf{F}_P^g$, etc. We have

$$\begin{aligned}
 \mathbf{F}_{\theta+\mathbf{O}\mathbf{X}}^g(\theta + \mathbf{O}\mathbf{x}) &= \mathbf{O}\mathbf{F}_X^g(\mathbf{x}) & \mathbf{x} \in \mathbb{R}^d, \\
 \mathbf{Q}_{\theta+\mathbf{O}\mathbf{X}}^g(\mathbf{O}\mathbf{u}) &= \theta + \mathbf{O}\mathbf{Q}_X^g(\mathbf{u}) & \mathbf{u} \in \mathbb{B}_d, \\
 \mathcal{R}_{\theta+\mathbf{O}\mathbf{X}}^g(\tau) &= \theta + \mathbf{O}\mathcal{R}_X^g(\tau) & \tau \in [0, 1), \quad \text{and} \\
 \mathcal{C}_{\theta+\mathbf{O}\mathbf{X}}^g(\tau) &= \theta + \mathbf{O}\mathcal{C}_X^g(\tau) & \tau \in [0, 1).
 \end{aligned}$$

In particular, if P enjoys symmetry properties (rotational, central, or with respect to some hyperplanes), \mathbf{F}_P^g , \mathbf{Q}_P^g , $\mathcal{R}_P^g(\tau)$, and $\mathcal{C}_P^g(\tau)$ enjoy *the same* symmetry properties as P for all $\tau \in [0, 1)$.

Recall that an essential property of distribution functions in dimension $d = 1$ is their non-decreasing monotonicity. In higher dimensions, the concept of monotonicity still makes sense; we distinguish two notions of monotonicity, which both reduce to the usual concept of (non-decreasing) monotonicity when $d = 1$: *monotonicity* and *cyclical monotonicity*. We say that a map $\mathbf{G} : \mathbb{R}^d \rightarrow \mathbb{R}^d$ is *monotone* if

$$(\mathbf{G}(\mathbf{y}) - \mathbf{G}(\mathbf{x}))'(\mathbf{y} - \mathbf{x}) \geq 0$$

for all $\mathbf{x}, \mathbf{y} \in \mathbb{R}^d$. We say that G is *cyclically monotone* if for any $m \geq 1$ we have

$$\sum_{k=1}^m (\mathbf{G}(\mathbf{x}_{k+1}) - \mathbf{G}(\mathbf{x}_k))' \mathbf{x}_{k+1} \geq 0$$

for every cycle $x_1, x_2, \dots, x_{m+1} := x_1$. For $m = 2$, cyclical monotonicity yields

$$(\mathbf{G}(\mathbf{x}_2) - \mathbf{G}(\mathbf{x}_1))' \mathbf{x}_2 + (\mathbf{G}(\mathbf{x}_1) - \mathbf{G}(\mathbf{x}_2))' \mathbf{x}_1 \geq 0,$$

and cyclical monotonicity thus implies monotonicity. Theorem 24.8 in Rockafellar (1970) essentially entails that \mathbf{G} is cyclically monotone precisely when it writes as the gradient $\mathbf{G} = \nabla \psi$ of some convex (potential) function $\psi : \mathbb{R}^d \rightarrow \mathbb{R}$.

The following then holds.

(vii) The maps \mathbf{F}_P^g and \mathbf{Q}_P^g are cyclically monotone, hence also monotone, over \mathbb{R}^d .

Indeed, similarly to the center-outward distribution functions based on measure transportation introduced in Section 2.1, geometric distribution functions are gradients of convex functions. This is clear from (7), which immediately yields $\mathbf{F}_P^g = \nabla \phi_P^g$, where

$$\mathbf{z} \mapsto \phi_P^g(\mathbf{z}) := \mathbb{E}[\|\mathbf{z} - \mathbf{X}\| - \|\mathbf{X}\|], \quad \mathbf{z} \in \mathbb{R}^d$$

is a convex function and $\mathbf{X} \sim P$. It follows that \mathbf{F}_P^g is cyclically monotone, which implies that its inverse \mathbf{Q}_P^g is cyclically monotone too (hence the gradient of a convex function).

However, the geometric distribution function \mathbf{F}_P^g , in general, does not push P forward to the spherical uniform U_d over \mathbb{B}_d . Would this be case, \mathbf{F}_P^g and \mathbf{F}_P^\pm both being gradients of convex functions, the a.s. uniqueness result of McCann (1955) would imply $\mathbf{F}_P^g = \mathbf{F}_P^\pm$ a.s. for all $P \in \mathcal{P}_d^+$ (see Section 2.2), which cannot hold in general. Indeed, \mathbf{F}_P^g can be defined as the solution of the previously mentioned *linear* PDE (see Konen (2022)), while \mathbf{F}_P^\pm can be defined as the solution of a PDE of the Monge-Ampère type which is *nonlinear* (see Hallin et al. (2021)). Therefore, the solutions \mathbf{F}_P^g and \mathbf{F}_P^\pm , for general P , do not coincide and \mathbf{F}_P^g , in general, does not push P forward to U_d .

Nevertheless, recalling that \mathbf{F}_P^g is a homeomorphism between \mathbb{R}^d and \mathbb{B}_d , we see that each point $\mathbf{x} \in \mathbb{R}^d$ belongs to exactly one geometric contour, namely $\mathbf{x} \in \mathcal{C}_P^g(\tau)$ where $\tau = \|\mathbf{F}_P^g(\mathbf{x})\|$. Therefore, we can relabel quantile regions so that, in the new labeling, the region associated with an order $\tau \in [0, 1)$ has P -probability content τ . For this purpose, it is enough to observe that the map

$$\tau \mapsto \kappa_P^g(\tau) := P[\mathcal{R}_P^g(\tau)], \quad \tau \in [0, 1),$$

from $[0, 1) \rightarrow [0, 1)$ is a continuous and monotone increasing bijection. In fact, κ_P^g is the univariate distribution function of the random variable $\|\mathbf{F}_P^g(\mathbf{X})\|$ with $\mathbf{X} \sim P$. Consequently, we can define the *relabelled geometric distribution function* of P (of $\mathbf{X} \sim P$) as

$$\mathbf{x} \mapsto \tilde{\mathbf{F}}_P^g(\mathbf{x}) := \mathbf{B}_P^g(\mathbf{F}_P^g(\mathbf{x})), \quad (11)$$

where

$$\mathbf{B}_P^g(\mathbf{x}) := \begin{cases} \kappa_P^g(\|\mathbf{x}\|) \frac{\mathbf{x}}{\|\mathbf{x}\|} & \text{if } \mathbf{x} \neq 0 \\ 0 & \text{if } \mathbf{x} = 0 \end{cases}$$

is a homeomorphism. Consequently, the relabeled geometric distribution function $\tilde{\mathbf{F}}_P^g$ is also a homeomorphism, hence continuously invertible: define the *relabeled geometric quantile function* as its inverse $\tilde{\mathbf{Q}}_P^g := (\tilde{\mathbf{F}}_P^g)^{-1}$. The collections of regions and contours associated with $\tilde{\mathbf{F}}_P^g$ are the same as those associated with \mathbf{F}_P^g —only the labels have changed. Call $\tilde{\mathcal{R}}_P^g(\tau) := \tilde{\mathbf{Q}}_P^g(\tau \mathbb{B}_d)$ the *relabeled geometric quantile region of order τ* . Then, $\tilde{\mathcal{R}}_P^g(\tau)$ satisfies the essential property of a quantile region of order τ :

- (viii) the relabeled geometric quantile region $\tilde{\mathcal{R}}_P^g(\tau)$ has P-probability content τ for all $\tau \in [0, 1)$, irrespective of P.

We similarly define the *relabeled geometric quantile contours*

$$\tilde{\mathcal{C}}_P^g(\tau) := \tilde{\mathbf{Q}}_P^g(\tau \mathbb{S}^{d-1}), \quad \tau \in [0, 1).$$

One may wonder whether $\tilde{\mathbf{F}}_P^g$ now coincides with \mathbf{F}_P^\pm (hence, $\tilde{\mathbf{Q}}_P^g$ with \mathbf{Q}_P^\pm). First, let us stress that, even though $\|\tilde{\mathbf{F}}_P^g(\mathbf{X})\|$, just like $\|\mathbf{F}_P^\pm(\mathbf{X})\|$, is uniformly distributed over $[0, 1)$ when $\mathbf{X} \sim P$, the behavior of $\mathbf{F}_P^g(\mathbf{X})/\|\mathbf{F}_P^g(\mathbf{X})\|$, to the best of our knowledge, remains unknown, and has not been investigated so far. Second, observe that \mathbf{B}_P^g writes as the gradient ∇h_P^g of the convex function

$$\mathbf{x} \mapsto h_P^g(\mathbf{x}) := \int_0^{\|\mathbf{x}\|} \kappa_P^g(s) ds, \quad \mathbf{x} \in \mathbb{R}^d.$$

It follows that $\tilde{\mathbf{F}}_P^g = \nabla h_P^g \circ \nabla \phi_P^g$. However, it is well known that the composition of two gradients of convex functions, in general, is not the gradient of a convex function. For these reasons, which do not constitute rigorous proofs, we believe that there is no obvious reason why the equality $\tilde{\mathbf{F}}_P^g = \mathbf{F}_P^\pm$ should hold for general P. The simulations in Section 5) below—which do not constitute mathematical proofs—actually suggest that $\tilde{\mathcal{R}}_P^g(\tau)$ and $\mathcal{R}_P^\pm(\tau)$, for some distributions P, very strongly differ.

4.2 Center-outward quantile regions and contours

Let $P \in \mathcal{P}_d^+$. It is shown in Hallin et al. (2021) that

- (i) the regions $\mathcal{R}_P^\pm(\tau)$ are compact and arc-connected for all $\tau \in (0, 1)$;
- (ii) the regions $\mathcal{R}_P^\pm(\tau)$ are strictly nested as τ increases: $\mathcal{R}_P^\pm(\tau_1) \subsetneq \mathcal{R}_P^\pm(\tau_2)$ for any $0 < \tau_1 < \tau_2 < 1$;
- (iii) the median region $\mathcal{R}_P^\pm(0)$ is compact, convex, and has Hausdorff dimension at most $(d - 1)$;

- (iv) if, for some $k \in \mathbb{N}$ and $\alpha \in (0, 1)$, the density of P is locally of class $C^{k,\alpha}$, then the contour $\mathcal{C}_P^\pm(\tau)$ is a $(d-1)$ -dimensional manifold of class $C^{k+1,\alpha}$ for all $\tau \in (0, 1)$;
- (v) for $d = 1$, \mathbf{F}_P^\pm , \mathbf{Q}_P^\pm , \mathcal{R}_P^\pm , and \mathcal{C}_P^\pm reduce to F_P^\pm , Q_P^\pm , \mathcal{R}_P^\pm , and \mathcal{C}_P^\pm .

Note that (iv) was first established in del Barrio et al. (2020) when the support of P is convex, then refined in del Barrio and González-Sanz (2023). By construction, we also have the following:

- (vi) the P -probability content of $\mathcal{R}_P^\pm(\tau)$ equals the U_d -probability content of $\tau \mathbb{B}_d$, which is τ : $\mathcal{R}_P^\pm(\tau)$ and $\mathcal{C}_P^\pm(\tau)$, thus, qualify as the center-outward quantile region and quantile contour of order τ of P ;
- (vii) if $\mathbf{X} \sim P$, then $\mathbf{F}_P^\pm(\mathbf{X}) \sim U_d$; if $\mathbf{U} \sim U_d$, then $\mathbf{Q}_P^\pm(\mathbf{U}) \sim P$: both \mathbf{F}_P^\pm and \mathbf{Q}_P^\pm , thus, fully characterize P .³
- (viii) the maps \mathbf{F}_P^\pm and \mathbf{Q}_P^\pm are cyclically monotone, hence monotone, over \mathbb{R}^d .

Finally, \mathbf{F}_P^\pm and \mathbf{Q}_P^\pm enjoy the following invariance/equivariance properties (see Hallin et al. (2022)).

- (ix) Let $\theta \in \mathbb{R}^d$ and denote by \mathbf{O} an arbitrary $d \times d$ orthogonal matrix. Letting $\mathbf{X} \sim P$, write \mathbf{F}_X^\pm , \mathbf{Q}_X^\pm , etc. for \mathbf{F}_P^\pm , \mathbf{Q}_P^\pm , etc. Then,

$$\begin{aligned}
 \mathbf{F}_{\theta+\mathbf{O}\mathbf{X}}^\pm(\theta + \mathbf{O}\mathbf{x}) &= \mathbf{O}\mathbf{F}_X^\pm(\mathbf{x}) & \mathbf{x} \in \mathbb{R}^d, \\
 \mathbf{Q}_{\theta+\mathbf{O}\mathbf{X}}^\pm(\mathbf{O}\mathbf{u}) &= \theta + \mathbf{O}\mathbf{Q}_X^\pm(\mathbf{u}) & \mathbf{u} \in \mathbb{B}_d, \\
 \mathcal{R}_{\theta+\mathbf{O}\mathbf{X}}^\pm(\tau) &= \theta + \mathbf{O}\mathcal{R}_X^\pm(\tau) & \tau \in [0, 1), \quad \text{and} \\
 \mathcal{C}_{\theta+\mathbf{O}\mathbf{X}}^\pm(\tau) &= \theta + \mathbf{O}\mathcal{C}_X^\pm(\tau) & \tau \in [0, 1).
 \end{aligned}$$

In particular, if P enjoys symmetry properties (rotational, central, or with respect to some hyperplanes), \mathbf{F}_P^\pm , \mathbf{Q}_P^\pm , $\mathcal{R}_P^\pm(\tau)$, and $\mathcal{C}_P^\pm(\tau)$ enjoy the same symmetry properties as P for all $\tau \in [0, 1)$. This is not the case for the distribution and quantile functions resulting from a transport to the Lebesgue uniform over the unit cube $[0, 1]^d$ which are favored by some authors.

These properties, which for dimension $d = 1$ reduce to those of F^\pm and Q^\pm and constitute the essence of the concepts of distribution and quantile functions, fully justify the terminology *center-outward distribution and quantile functions* for \mathbf{F}_P^\pm and \mathbf{Q}_P^\pm . The *only* difference, here, between the properties of \mathbf{F}_P^\pm and \mathbf{Q}_P^\pm and those of \mathbf{F}_P^g and \mathbf{Q}_P^g is (vi) above, and this difference disappears if the relabeled functions $\tilde{\mathbf{F}}_P^g$ and $\tilde{\mathbf{Q}}_P^g$ are substituted for \mathbf{F}_P^g and \mathbf{Q}_P^g , respectively.

In view of this, the relabeled geometric and the center-outward concepts, which, it seems, do not coincide, apparently both qualify as equally satisfactory multivariate concepts of distribution and quantile functions. Is there a way to break that tie and select one of them rather than the other? Since analytical expressions are impossible,

³ Note, however, that the collections of center-outward regions or center-outward contours alone (that is, without the mappings \mathbf{F}_P^\pm or \mathbf{Q}_P^\pm between \mathbb{R}^d and \mathbb{B}_d) do not characterize P .

one has to recur to numerical approximations—in statistical terms, simulations—in order to perform comparisons. This is what we are doing in the next section, where comparisons are based on simulations of the quantile contours $\mathcal{G}_P^\pm(\tau)$ and $\mathcal{G}_P^g(\tau)$.

5 Geometric and center-outward quantile contours: an empirical comparative study

5.1 Numerical computation of contours

Except for some very special distributions, such as the spherical ones, geometric and center-outward quantiles in dimension $d \geq 2$, unfortunately, are sharing the inconvenient absence of analytical expressions. Numerical solutions are possible, though, based on simulations with high numbers of replications. For all $N \in \mathbb{N}$, denote by P_N the empirical distribution of a random sample of size N drawn from P . The accuracy of these numerical solutions relies on consistency results for the empirical counterparts $\mathbf{F}_{P_N}^g$ and $\mathbf{Q}_{P_N}^g$ in the geometric case (obtained by substituting P_N for P in (7)), for $\mathbf{F}_{P_N}^\pm$ and $\mathbf{Q}_{P_N}^\pm$ in the measure-transportation setting (see Hallin et al. (2021) for precise definitions and details).

In the geometric case, Mottonen et al. (1997) established a Glivenko-Cantelli result of the form

$$\sup_{\mathbf{z} \in \mathbb{R}^d} \|\mathbf{F}_{P_N}^g(\mathbf{z}) - \mathbf{F}_P^g(\mathbf{z})\| \rightarrow 0 \quad (12)$$

with P -probability one as $N \rightarrow \infty$, provided that P admits a bounded density. In fact, one can show that the bounded density assumption is superfluous: similarly to distribution functions in dimension $d = 1$, the Glivenko-Cantelli result (12) is valid for an *arbitrary* probability measure. The same convergence holds for the sequence of relabeled counterparts $\tilde{\mathbf{F}}_P^g$ of \mathbf{F}_P^g and $\tilde{\mathbf{F}}_{P_N}^g$ of $\mathbf{F}_{P_N}^g$; see Konen (2022).

In the measure transportation approach, Hallin et al. (2021) proved a similar Glivenko-Cantelli result for an interpolated version $\bar{\mathbf{F}}_{P_N}^\pm$ of their empirical center-outward distribution functions $\mathbf{F}_{P_N}^\pm$:

$$\sup_{\mathbf{z} \in \mathbb{R}^d} \|\bar{\mathbf{F}}_{P_N}^\pm(\mathbf{z}) - \mathbf{F}_P^\pm(\mathbf{z})\| \rightarrow 0$$

with P -probability one as $N \rightarrow \infty$, when $P \in \mathcal{P}_d^+$ (see Section 2.2 for the definition of \mathcal{P}_d^+).

5.2 Numerical comparisons of quantile contours

Figure 1 shows, for orders $\tau \in \{.25, .50, .75\}$, plots of the empirical contours $\tilde{\mathcal{E}}_{P_N}^g(\tau)$ and $\mathcal{E}_{P_N}^\pm(\tau)$ based on random samples $\mathbb{X}_N = \{\mathbf{X}_1, \dots, \mathbf{X}_N\}$ of size $N = 2,400$ from four different probability distributions on \mathbb{R}^2 . Given the regular grid

$$\left\{ \mathbf{u}_k = (\cos(\theta_k), \sin(\theta_k)) : \theta_k = \frac{2k\pi}{70} \text{ and } 1 \leq k \leq K \right\}$$

of directions on \mathbb{S}^1 , with $K = 70$, each contour $\tilde{\mathcal{E}}_{P_N}^g(\tau)$ is estimated by

$$\left\{ \tilde{\mathbf{Q}}_{P_N}^g(\tau \mathbf{u}_k) : 1 \leq k \leq K = 70 \right\},$$

where $\tilde{\mathbf{Q}}_{P_N}^g$ stands for the relabeled geometric quantile map defined in Section 3.1. In other words, to each level τ we first associate the level τ' such that

$$\tilde{\mathcal{E}}_{P_N}^g(\tau) = \mathcal{E}_{P_N}^g(\tau').$$

Then, the geometric contour $\mathcal{E}_{P_N}^g(\tau')$ is obtained as the collection $\{\mathbf{z}_1, \dots, \mathbf{z}_K\}$ such that \mathbf{z}_k minimizes the empirical objective function $O_{\tau', \mathbf{u}_k}^{P_N}$.

Each measure-transportation-based contour is estimated by

$$\left\{ \mathbf{Q}_{P_N}^\pm(\tau \mathbf{u}_k) : 1 \leq k \leq K \right\}.$$

To construct the map $\mathbf{Q}_{P_N}^\pm$, we first fix a regular $n_R \times n_S$ grid \mathcal{G}_N over the punctured unit ball $(0, 1) \times \mathbb{S}^1$ such that $n_R n_S = N$;⁴ our simulation relies on $N = 2,400$ replications, with $n_R = 40$ and $n_S = 60$. Then, we seek an optimal coupling between \mathbb{X}_N and \mathcal{G}_N , i.e., we associate to each $\mathbf{X}_k \in \mathbb{X}_N$ a unique $\mathbf{F}_{P_N}^\pm(\mathbf{X}_k) \in \mathcal{G}$ in such a way that

$$\sum_{k=1}^N \|\mathbf{X}_k - \mathbf{F}_{P_N}^\pm(\mathbf{X}_k)\|^2 = \min_{\pi \in \Pi} \sum_{k=1}^N \|\mathbf{X}_{\pi(k)} - \mathbf{F}_{P_N}^\pm(\mathbf{X}_k)\|^2,$$

where π ranges over the set Π of permutations of $\{1, \dots, N\}$. A continuous map $\bar{\mathbf{F}}_{P_N}^\pm$ then is obtained from the values $\mathbf{F}_{P_N}^\pm(\mathbf{X}_k)$ of $\mathbf{F}_{P_N}^\pm$ at \mathbf{X}_k by interpolation techniques; see Hallin et al. (2021) for further details.

These samples were generated from

- (i) the centered bivariate normal distribution with covariance matrix $\Sigma = \begin{pmatrix} 2 & 1 \\ 1 & 1 \end{pmatrix}$;
- (ii) the bivariate distribution with independent exponential marginals with mean one;

⁴ In the case of a genuine sample, N is factorized into $N = n_R n_S + n_0$ with $n_0 < \min(n_R, n_S)$. We refer to Hallin and Mordant (2023) for details on the choice of n_R and n_S . Here, however, we are dealing with simulations, and can choose N such that $n_0 = 0$.

- (iii) the standard skew- t distribution with four degrees of freedom and slant vector $\alpha = (10, 10)$ — see Azzalini and Capitanio (2014)—and
- (iv) the banana-shaped distribution considered in Hallin et al. (2021), viz. the mixture

$$\frac{3}{8}\mathcal{N}(\mu_1, \Sigma_1) + \frac{3}{8}\mathcal{N}(\mu_2, \Sigma_2) + \frac{1}{4}\mathcal{N}(\mu_3, \Sigma_3),$$

of three bivariate normal distributions where

$$\mu_1 = \begin{pmatrix} -3 \\ 0 \end{pmatrix}, \quad \mu_2 = \begin{pmatrix} 3 \\ 0 \end{pmatrix}, \quad \mu_3 = \begin{pmatrix} 0 \\ -\frac{5}{2} \end{pmatrix},$$

and

$$\Sigma_1 = \begin{pmatrix} 5 & -4 \\ -4 & 5 \end{pmatrix}, \quad \Sigma_2 = \begin{pmatrix} 5 & 4 \\ 4 & 5 \end{pmatrix}, \quad \Sigma_3 = \begin{pmatrix} 4 & 0 \\ 0 & 1 \end{pmatrix}.$$

Inspection of Figure 1 reveals the following facts.

- (a) First, the contours obtained by measure transportation seem to better reflect the geometry of the underlying distributions. This is particularly obvious for the banana-shaped distribution (iv), where the concave shape of the mixture is well picked up by the center-outward contours but completely missed by the relabeled geometric ones. The same phenomenon also takes place, to a less spectacular extent, under distributions (i)-(iii): the relabeled geometric quantile region of order .75, under the exponential distribution (ii), largely extends beyond the exponential support, something the center-outward contours do not; the same geometric contours, for the skew- t distribution (iii), contrary to the center-outward ones, hardly exhibit any skewness.
- (b) Second, while relabeled geometric quantiles (as a direct consequence of their re-labelization rather than because of their L_1 characterization) do provide the desired control over the probability content of their regions, hence yield, for each $\mathbf{X}_i \in \mathbb{X}_N$, a sound concept $R_i^{(N)} := \text{rank}(\|\mathbf{F}_{\mathbf{P}_N}^{\text{eg}}(\mathbf{X}_i)\|)$ of center-outward multivariate rank, they do not provide any clear notion of signs. Such signs, quite on the contrary, are well defined, in the measure-transportation-based approach, for the sample points $\mathbf{X}_i \in \mathbb{X}_n$, as the unit vectors $\mathbf{F}_{\mathbf{P}_N}^{\pm}(\mathbf{X}_i)/\|\mathbf{F}_{\mathbf{P}_N}^{\pm}(\mathbf{X}_i)\|$, $i = 1, \dots, N$, which are i.i.d. (uniform over the unit vectors associated with the N gridpoints in \mathfrak{G}_N and independent of the ranks $R_1^{(N)}, \dots, R_N^{(N)}$).
- (c) On the other hand, geometric contours are more regular than their measure-transportation-based counterparts. This is a consequence of (iii) and (iv) in Sections 3.1 and 3.2, respectively: geometric contours are continuous as soon as \mathbb{P} is non-atomic and smooth (at least C^{d-1}) while the oscillations, hence also the variability, of the interpolated measure-transportation-based contours are further increased by the interpolation scheme.

While points (a) and (b) above are pleading for the measure-transportation-based concepts, the decisive argument in favor of the latter follows from a theoretical result

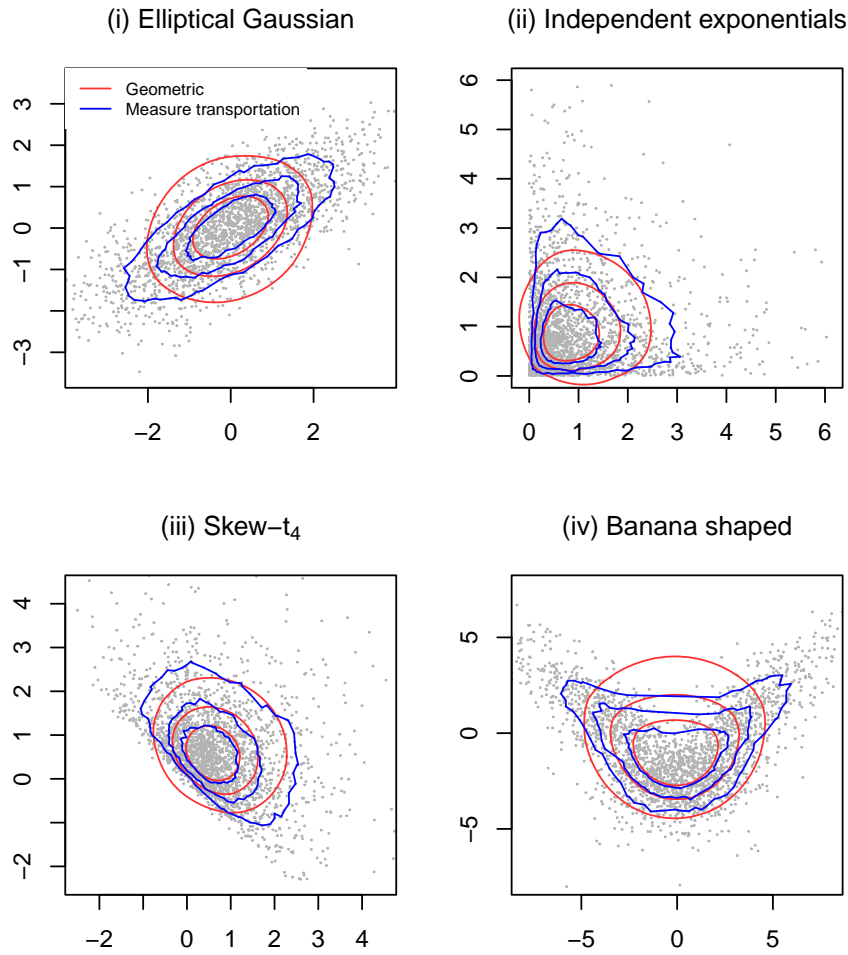


Fig. 1 Geometric (red) and measure-transportation-based (blue) contours of levels $\tau = .25, .5, .75$ for samples of size $N = 2400$ drawn from four different distributions. Geometric contours are re-labeled according to their probability content, and measure-transportation contours are obtained through the interpolation scheme (see Hallin et al. (2021)) of the optimal coupling between the observations and a 40×60 regular grid \mathcal{G}_N of the unit ball in \mathbb{R}^2 ; see Section 4.2 for details. Empirical quantiles, both geometric and center-outward, are connected by lines in the plots.

by Girard and Stupfler (2017) on the “intriguing behavior” (a clear understatement) of high-order geometric quantile contours.

5.3 Numerical comparison of extreme contours

Girard and Stupfler (2017) establish the following disturbing result for extreme geometric quantiles: if P is a probability measure on \mathbb{R}^d with finite second-order moments, i.e. $E_P[\|\mathbf{X}\|^2] < \infty$ for $\mathbf{X} \sim P$ with covariance matrix Σ , then, denoting by $\text{Tr}(\mathbf{A})$ the trace of a square matrix \mathbf{A} ,

$$\|\mathbf{Q}_P^g(\tau\mathbf{u})\|^2(1-\tau) \rightarrow \frac{1}{2} \left(\text{Tr} \Sigma - \mathbf{u}'\Sigma\mathbf{u} \right)$$

as $\tau \rightarrow 1$ for any $\mathbf{u} \in \mathbb{S}^{d-1}$. First, let us stress that the quantity $\text{Tr} \Sigma - \mathbf{u}'\Sigma\mathbf{u}$ is always non-negative, and is strictly positive as soon as Σ is non-degenerate. In addition to providing the rate at which extreme geometric quantiles are “escaping to infinity,” this result also provides valuable insights on the shape of the corresponding extreme contours. For instance, taking for \mathbf{u} a unit eigenvector \mathbf{u}_{\max} associated with Σ 's *largest* eigenvalue yields a norm $\|\mathbf{Q}_P^g(\tau\mathbf{u}_{\max})\|$ for the contour $\mathcal{C}_P^g(\tau)$ of order τ in direction \mathbf{u} which is *minimal* for $\tau \rightarrow 1$; the same contour, in the direction \mathbf{u}_{\min} associated with the smallest eigenvalue of Σ , asymptotically yields the *largest* norm $\|\mathbf{Q}_P^g(\tau\mathbf{u}_{\min})\|$. More generally, due to the fact that the shape factor $\text{Tr} \Sigma - \mathbf{u}'\Sigma\mathbf{u}$ is a decreasing function of $\mathbf{u}'\Sigma\mathbf{u}$, the asymptotic behavior of extreme quantiles—moving away fast from the center along the eigendirections of Σ associated with small eigenvalues, and slowly along the eigendirections of Σ associated with large eigenvalues—is exactly the opposite of what it is expected to be. This is highly counterintuitive and, actually, totally unacceptable.

Figure 2 provides a finite-sample empirical illustration of this theoretical fact. We generated a sample of size $N = 1,000$ from a centered bivariate Gaussian distribution $\mathcal{N}(\mathbf{0}, \Sigma)$ with covariance matrix $\Sigma = \begin{pmatrix} 1/8 & 0 \\ 0 & 3/4 \end{pmatrix}$. Then, for $\tau \in \{.90, .95, .99\}$, we computed the empirical relabeled geometric and transportation-based quantile contours of order τ , as described in Sections 5.1 and 5.2, with $K = 50$, $n_R = 20$, and $n_S = 50$ for the latter (see Section 5.2 for notation).

Figure 2 perfectly illustrates the pathological phenomenon described by Girard and Stupfler (2017): the geometric contours are much wider in the (horizontal) directions associated with Σ 's smaller eigenvalue, and narrower in the (vertical) directions associated with Σ 's larger eigenvalue. This pathological behaviour is increasingly severe as τ approaches one: for $\tau = .90$, the contour is approximately circular. In sharp contrast, the center-outward contours, irrespective of τ , are correctly accounting for the shape of the distribution and the relative magnitudes of Σ 's eigenvalues.

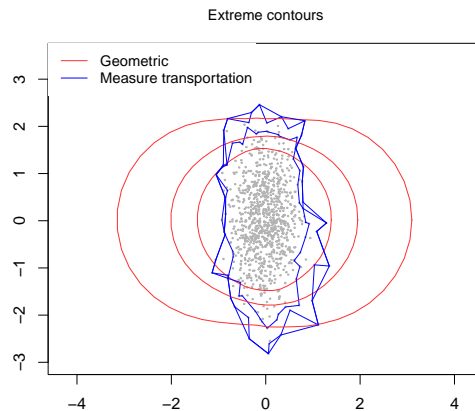


Fig. 2 Geometric (red) and measure-transportation-based (blue) contours of order $\tau = .90, .95, .99$ for samples of size $N = 1,000$ drawn from a (nonspherical) bivariate Gaussian distribution on \mathbb{R}^2 . Empirical quantiles, both geometric and center-outward, are connected by lines in the plots.

6 Conclusions

Among all concepts of multivariate quantiles proposed in the literature, geometric quantiles (after due re-labelization) and measure-transportation-based center-outward quantiles are the most convincing ones: they both reduce to classical concepts in dimension one, and both satisfy most properties expected from quantiles, quantile regions, and quantile contours. Empirical comparisons and a highly pathological property of extreme geometric quantiles established by Girard and Stupfler (2017), however, are tilting the balance in favour of the measure-transportation-based concept.

Acknowledgments

Marc Hallin acknowledges the support of the Czech Science Foundation grant GAČR22036365. Dimitri Koenen is supported by a research fellowship from the Centre for Research in Statistical Methodology (CRiSM) of the University of Warwick. We thank Eustasio del Barrio and Alberto González-Sanz for kindly providing their codes for the computation of center-outward quantile functions and contours.

References

- Azzalini, A. and A. Capitanio (2014). *The Skew-Normal and Related Families*. IMS Monograph series. Cambridge University Press.
- Chaudhuri, P. (1996). On a geometric notion of quantiles for multivariate data. *Journal of the American Statistical Association* 91, 862–872.
- del Barrio, E. and A. González-Sanz (2023). Regularity of center-outward distribution functions in non-convex domains. *arXiv preprint arXiv:2303.16862*.
- del Barrio, E., A. González-Sanz, and M. Hallin (2020). A note on the regularity of optimal-transport-based center-outward distribution and quantile functions. *Journal of Multivariate Analysis* 180, 104671.
- Figalli, A. (2018). On the continuity of center-outward distribution and quantile functions. *Nonlinear Analysis* 177, 413–21.
- Girard, S. and G. Stupfler (2017). Intriguing properties of extreme geometric quantiles. *REVSTAT* 15, 107–139.
- Hallin, M., E. del Barrio, J. Cuesta-Albertos, and C. Matrán (2021). Distribution and quantile functions, ranks and signs in dimension d : a measure transportation approach. *Annals of Statistics* 49, 1139–1165.
- Hallin, M. and G. Mordant (2023). On the finite-sample performance of measure-transportation-based multivariate rank tests. In M. Yi and K. Nordhausen (Eds.), *Robust and Multivariate Statistical Methods: Festschrift in Honor of David E. Tyler*, pp. 87–119. Springer.
- Koltchinski, V. (1997). M-estimation, convexity and quantiles. *Annals of Statistics* 25, 435–477.
- Konen, D. (2022). Recovering a probability measure from its geometric cdf. *arXiv preprint arXiv:2208.11551*.
- Konen, D. and D. Paindaveine (2022). Multivariate ρ -quantiles: a spatial approach. *Bernoulli*, 28, 1912–1934.
- McCann, R. J. (1995). Existence and uniqueness of monotone measure-preserving maps. *Duke Mathematical Journal* 80, 309–323.
- Mottonen, J., H. Oja, and J. Tienari (1997). On the efficiency of multivariate spatial sign and rank tests. *Annals of Statistics* 25, 542–552.
- Paindaveine, D. and J. Virta (2020). On the behavior of extreme d -dimensional spatial quantiles under minimal assumptions. In A. Daouia and A. Ruiz-Gazen (Eds.), *Advances in Contemporary Statistics and Econometrics*, pp. 243–259. Springer.
- Rockafellar, R. T. (1970). *Convex Analysis*. Princeton Mathematical Series. Princeton University Press.